Received: 4 September 2023 | Revised: 1 January 2024 | Accepted: 3 January 2024

DOI: 10.1002/btpr.3429

RESEARCH ARTICLE

Cell Culture and Tissue Engineering

BIOTECHNOLOGY PROGRESS

# Implementation of mDoE-methods to a microcarrier-based expansion processes for mesenchymal stem cells

Kim B. Kuchemüller | Ralf Pörtner | Johannes Möller

Institute of Bioprocess and Biosystems Engineering, Hamburg University of Technology, Hamburg, Germany

**Correspondence**
Johannes Möller, Hamburg University of Technology, Institute of Bioprocess and Biosystems Engineering, Denickestraße 15, 21073 Hamburg, Germany.
Email: johannes.moeller@tuhh.de

## Abstract

The need for advanced therapy medicinal products (ATMPs) has gained increased attention in recent years. In this respect, a well-designed cell expansion process is needed to efficiently manufacture the required number of cells with the desired product quality. This step is challenging due to the biological complexity of the respective primary cell (e.g., mesenchymal stem cells (MSC)) and the usage of microcarrier-based expansion systems. One accelerating approach for process design is model-assisted Design of Experiments (mDoE) combining mathematical process models and statistical tools. In this study, the mDoE workflow was used for the development of an expansion processes with human immortalized mesenchymal stem cells (hMSC-TERT) and the aim of maximizing cell yield assuming only a limited amount of prior knowledge at a very early stage of development. First, suitable microcarriers for expansion in shake flasks were screened and the differentiation of the cells was proven. Second, initial experiments were performed to generate prior knowledge, which was then used to set up the mathematical model and to estimate the model parameters. Finally, the mDoE was used to determine and evaluate the design space to be performed experimentally. Overall, a cell expansion process using microcarriers in a shake flask culture was successfully implemented and a significant increase in cell yield (up to 6,2-fold) was achieved compared to literature.

**KEYWORDS**

bioprocess modeling, early stage development, hMSC-TERT, microcarrier culture, model-assisted Design of Experiments, process design

## 1 | INTRODUCTION

Advanced therapy medicinal products (ATMPs), which are divided into gene and cell therapeutics and tissue engineered products, have gained increased attention in recent years.[1–3] Gene and cell therapeutics are already being investigated in numerous clinical trials for a range of diseases, including cancer, brain injuries, and chronic infections.[4–6] Cells applied in cell therapy comprise mesenchymal stem cells, T lymphocytes, tumor-infiltrating lymphocytes, chimeric antigen

**Abbreviations:** Amm, ammonia; ATMP, advanced therapy medicinal products; CAR, Chimeric antigen receptor; DAPI, 4′,6-diamidine-2-phenylindole; DMEM, Dulbecco's Modified Eagle Medium; DoE, Design of Experiments; EDTA, ethylendiaminetetraacetic acid; Glc, glucose; Gln, glutamine; hMSC-TERT, human immortalized mesenchymal stem cells; ISCT, International Society for Stem Cell Research; Lac, lactate; LS, limiting substrate; MC, microcarrier; mDoE, model-assisted DoE; OFAT, one-factor-at-a-time; PBS, phosphate-buffered saline; SG, SYBR GREEN I.

receptor T-cells, natural killer cells, among others, to some extend genetically modified (e.g., Chimeric antigen receptor (CAR)-engineered T-cells).[7–9] Tissue engineered products are a biological medicinal product that contains bioengineered cells or tissues or consists of the latter.[10–12] However, the novelty of ATMPs is accompanied by special challenges in their development, the design of a manufacturing process and the regulatory approval. The final in vivo therapeutic efficacy of cell products depend to a large extend on the manufacturing process.[13,14] Within the mostly patient specific manufacturing workflow,[15] generation of the required amount of cells, comprising clinical-grade purification and ex vivo expansion, preferably in accordance with quality manufacturing guidelines (current Good Manufacturing Practice, ICH Guidelines) are crucial.[7,13,14,16–19] This represents a major challenge especially for cell and gene therapy, as final cell product doses up to 50–100 billion T-cells are required.[20] Therefore, the focus here will be on cell expansion for this purpose.

Techniques used for cell expansion have been reviewed extensively by References [15]. In brief, on a smaller scale, static culture dishes (e.g., well plates, T-flasks, stacked plate systems, mostly single-use) are mainly used for cell expansion. For these systems monitoring and control of parameters such as temperature, pH, and oxygen supply can be difficult. Moreover, the typical cell concentrations (25,000–30,000 cells/cm$^2$) provided by common planar cultivation systems with up to 40 layers cannot achieve the desired cell numbers (e.g., > billions of cells per batch required for cell therapy) and consistent quality, even with a high degree of automation and parallelization.[21,22] As plates and flasks allow for a limited expansion only, scalable bioreactor systems based on matrices to provide cell attachment have been established in the past. These cover hollow fiber bioreactors, bioreactors for macrocarriers (e.g., fixed bed), meander type bioreactors, and, microcarriers for use in stirred tank reactors, either re-usable or single use (reviewed by[23]). Although stirred tank reactors operated with microcarriers have shown promising results, they were originally designed for mammalian cell-based productions of therapeutic proteins.[24] However, stem cells are less robust and more sensitive than the therapeutic production cells.[25] In addition, the stem cell culture media differ in compositions, particularly in their supplements, and serum (up to 20%) is usually present.[26,27]

With respect to the before mentioned requirements, the stem cell expansion processes needs to be standardized based on the process understanding with a special focus on process robustness and scalability to ensure the desired product quality.[7,9,28] However, this requires immense efforts during process development, industrial implementation and transfer with challenging development procedures and long timelines.[29] During process development, specifically dedicated to the cell number required for clinical application, trial-and-error and one-factor-at-a-time (OFAT) methods are still "state of the art". However, these inevitably require a large number of experiments to be performed and analytically evaluated.[30,31] The alternative use of statistical Design of Experiments (DoE) methods offers the possibility of additionally identifying cause-effect-relationships between process parameters and their influence on final cell density, but nevertheless reduces the complex bioprocess to a few metrics (e.g., final cell concentration) and does not sufficiently account for the dynamics of growth and metabolism.[32–34] At the same time, there is a risk that experiments are incorrectly selected by the heuristic design of a DoE, having insufficient explanatory power. This additionally increases costs and leads to time delays.[32,35,36]

A more advanced approach for the reduction of development times and the related costs of cell propagation processes is the combination of mathematical growth models with statistical optimization methods, called mDoE.[37] In mDoE, the process understanding is captured in a mathematical model which is used to evaluate experimental designs in silico before they are performed in the laboratory. Recommended experiments are thus implemented experimentally in a significantly reduced number and product quality and quantity can be better ensured.[33,38] The successful application of mDoE has been demonstrated for the optimization of medium and feeding strategies for antibody-producing mammalian cell culture and *Saccharomyces cerevisiae* expansion processes including a whole-cell biocatalysis.[32,33] Additionally, the use of mathematical process models is nowadays seen as a sustainable part of process development. This has been discussed extensively for production of recombinant therapeutic proteins (e.g., antibodies).[37,39,40] Examples for model-assisted development of cell therapeutics and tissue engineered products have been recently reviewed by References [15,41].

Recently, we showed the successful application of mDoE for the development of an expansion process for an adherent cell line (L929).[42] Additionally, a mathematical model to describe cell growth of adherent cells on microcarriers was presented.[42] Based on the previous developments, the intention of this study was to evaluate, if the mDoE workflow is beneficial for the development of expansion processes for ATMPs. As test system, an expansion process for hMSC-TERT cells was developed with the aim of maximizing cell yield assuming only a limited amount of prior knowledge at a very early stage of development. In this respect, the mDoE-assisted workflow for process development for an ATMP cell line includes the following elements: choice of microcarriers, relevant analytical quality control of the cell line differentiation, model set-up and calibration. Building on these results, the design space will be elaborated with a special focus on bead-to-bead transfer. Following these specific tasks, suitable microcarriers for expansion in shake flasks were screened first and the differentiation of the cells according to ISCT-guidelines was proven. Second, initial experiments were performed to generate prior knowledge and determine cause-effect relationships, which was then used to set-up the mathematical model and to determine kinetic parameters. Finally, the mDoE was used to determine and evaluate the design space to be performed experimentally.

A critical step for the chosen microcarrier-based cell expansion is the transfer of cells between different scales, which is often accomplished by bead-to-bead-transfer. Design of this critical process step usually requires significant experimental effort. The mDoE was used to determine the start time of the bead-to-bead transfer and the concentration of MC in the bead-to-bead transfer focusing on a maximum cell concentration, first in silico to determine a suitable design space for the required experiments and then experimentally for verification. For the design of the cell expansion process the previously published mDoE software toolbox was used.[33,42]

## 2 | MATERIALS AND METHODS

### 2.1 | Cell lines, pre-cultivation and passaging in T-flasks

Adherent-growing hMSC-TERT cells (kindly provided by Prof. M. Kassem, University of Southern Denmark, Denmark and Prof. D. Salzig, Technical University of Applied Sciences Mittelhessen, Germany) were cultivated in static (e.g., T-flasks) and in dynamic (e.g., shaken) bioreactors. For the static cultivations, cryo-cultures containing $1 \times 10^6$ cells were thawed and transferred to 10 mL phosphate-buffered saline (PBS) (Carl Roth, Germany). The cell suspension was centrifuged for 4 min at 200*g* (Avanti J-26SXP, Beckmann Coulter, USA) and the supernatant was removed. The cell pellet was re-suspended in pre-warmed Dulbecco's Modified Eagle Medium (DMEM) (PAN-Biotech GmbH, Germany) and transferred to a cell culture T-flask (Greiner Bio-One, Austria) at a seed density of 5000 cells $cm^{-2}$ in DMEM with 10 vol% FBS (FBS Superior, Biochron GmbH, Germany). The cells were cultivated at 37°C and 5 vol% $CO_2$ in an incubator (HeraCell 150i, Thermo Fisher, USA). Depending on the experimental setup, the glucose (Sigma-Aldrich, USA) and glutamine (Lonza Group AG, Switzerland) concentrations were adjusted in the medium.

Reaching a confluence of 80%–90%, the cells were proteolytically solubilized from the growth surface with 1 vol% trypsin (Lonza Group AG, Switzerland) in PBS. For this, the medium was removed, and the T-flask was washed twice with PBS ($V_{PBS} = V_{medium}$). Then, the trypsin solution was applied and incubated for 5–7 min. Enzymatic proteolysis was stopped by the addition of medium ($V_{Trypsin} = V_{medium}$), so that new cultivation systems were subsequently inoculated with the obtained cell solution.

### 2.2 | Cultivation in shake flasks

Dynamic cultivations were performed in shake flasks (glass, Schott AG, USA) with working volumes of 25, 40, and 60 mL cultivation medium (DMEM; same as in Section 2.1) and different types and concentrations of microcarriers (MC). hMSC-TERT were inoculated at a cell density of 5000 cells $cm^{-2}$ of microcarriers, as low attachment densities are recommended for this cell type.[18,43,44] The shake flasks were incubated for one night without agitation at the beginning and subsequently the shaker speed (GFL 3005, GFL, Germany) was set to 60 rpm (shaking diameter = 10 mm). For bead-to-bead-transfer, 100% fresh medium and 25%, 50%, 75% or 100% fresh MC were added after 3, 5 or 7 days.

### 2.3 | Microcarriers and vessel siliconization

As microcarriers, Cytodex 3 (GE HealthCare, USA) and SoloHill (Sartorius, Germany) microcarriers were investigated. SoloHill MCs included Hillex II, Plastic, PlasticPlus, StarPlus, FACT III, and Collagen-Coated. Microcarriers were prepared as described in the manufacturers' protocols.

Siliconization of all glass culture vessels (shake flasks and bioreactor) was necessary to avoid adhesion of the microcarriers and cells to the vessel wall. For this purpose, a few mL of Sigmacote (Sigma-Aldrich, USA) were transferred to the respective vessel under a fume hood and rotated and swirled at regular intervals to distribute the solution. The respective vessel was then rinsed with ultrapure water and dried overnight in a 60°C heating oven (Thermo Scientific Heratherm, ThermoFisher Scientific, USA).

### 2.4 | Analytics

#### 2.4.1 | Cell harvest and lysis

For the enzymatic as well as cell lysing methods, 1 mL sample was taken, and the MCs were sedimented (1–3 min, depending on the respective MC). The supernatant was collected and stored for suspension cell count determination. Subsequently, the respective MC cell pellet was washed two times with PBS or with PBS + 2 mmol $L^{-1}$ Ethylendiaminetetraacetic acid (EDTA). Samples were incubated with enzyme solution for 5–7 min. The first enzyme solution is based on a 1 vol% trypsin mixture in PBS, while the second is composed of a 1:1 mixture of 0.25 vol% trypsin in PBS and 0.02 vol% EDTA in PBS. Further instructions can be found in Reference [15]. For the IGEPAL method, the protocol from Reference [16] was adopted, but no sieve was used.

#### 2.4.2 | Cell counting

Cell nuclei were stained by propidium iodide (Sigma-Aldrich, USA) and quantified using a flow cytometer (CytoFLEX, Beckman Coulter, USA) with the 585/42 filter and a 488 nm laser. Debris were excluded using SSC-A versus FSC-A gating and doublets were excluded with FSC-H versus FSC-A gating.

A Z2 Coulter Particle Count and Size Analyzer (Beckmann Coulter, USA) was used for cell counting. For measuring, a total volume of 10 mL was diluted with PBS and 2 mmol $L^{-1}$ EDTA according to the expected cell concentration. For quantification of fluorescence by the SYBR Green I (SG) (Sigma-Aldrich, USA) method, samples were centrifuged for 4 min at 200*g*, and the supernatant was removed and replaced with PBS. Subsequently, fluorescence measurements were performed in a black 96-well plate (Corning, Germany) threefold using a microplate reader (Tecan Infinite Nano+, Tecan, Switzerland). Further details can be found in Reference [17].

#### 2.4.3 | Determination of the distribution of cells on microcarriers

Fluorescence staining with 4′,6-diamidine-2-phenylindole (DAPI) (Carl Roth, Germany) was performed to assess cell growth on MCs.

Samples were centrifuged at 200*g* for 3 min and washed with PBS. The centrifugation step was then repeated, and the samples resuspended in 70 vol% ethanol. Intermediate storage was performed in a −20°C freezer (Bauknecht, Germany).

For microscopy, the ethanol supernatant of the samples was removed and replaced with PBS + 1 vol% Triton X-100 + 0.1 vol% DAPI. The fluorescent dye was incubated at room temperature in the dark for a period of 5 min. Subsequently, 50 µL of sample was pipetted onto a slide with coverslip. Microscopy was performed at 358 nm using a violet filter on the Eclipse 80i fluorescence microscope.

### 2.4.4 | Quantification of glucose, glutamine, lactate and ammonia

Concentrations of glucose ($c_{Glc}$), glutamine ($c_{Gln}$), and lactate ($c_{Lac}$) were measured with the YSI 2900D (Yellow Springs Instruments) biochemistry analyzer. The concentration of ammonium ($c_{Amm}$) was determined with an enzymatic test kit (AK00091; NZYTech, Portugal).

## 2.5 | Differentiation and characterization of hMSC-TERT

For differentiation and characterization, hMSC-TERT of different passages (40+ and 88+) were used. The ability of the cells for specialization was checked after static as well as dynamic cultivation. Differentiation kits from Miltenyi Biotec (Germany) were used for differentiation studies. Cells were prepared and treated as described in the manual, with deviations listed below.

To initiate adipogenesis and osteogenesis, cells were differently seeded in a ClipMax (Faust, Switzerland) as stated in the protocol. Additionaly, cells for adipogenesis were cultivated in standard cell culture medium and replaced with adipogenesis differentiation medium after an incubation period of 48 h. Finally, cells were cultivated for 13–28 days, with medium changes every 2–3 days. For osteogenic differentiation, cells were incubated for 14–21 days in osteogenic differentiation medium. Medium was changed every 2–3 days. The formation of a bone matrix as a result of calcium accumulation was confirmed by alizarin red staining after ethanol fixation. Chondrogenesis was stained with Alcian blue and nuclear red stain. For better visualization of the cartilage, sections of the nodules were prepared in advance.

To detect the surface markers of hMSC-TERT, an MSC phenotyping kit from Miltenyi Biotec was used. The integrated CD73-APC conjugate was replaced with a CD73-PE conjugate. The respective sample was labeled with the phenotyping cocktail and measured in CytoFLEX using 585/42, PB450, FITC and KOS525 filters at 488 nm. Simultaneously, one sample each was prepared as an isotype control and measured to determine non-specific binding.

## 2.6 | Mathematical methods

### 2.6.1 | Mathematical process model and estimation of model parameters

The mathematical model to describe the growth behavior of adherent-growing cells on microcarriers is described in Reference [42]. In brief, the model is based on our experience in modeling suspension-growing mammalian cell lines (see References [45] and [32]). The main advantage of this model is the modeling of the initial attachment phase of cells onto the microcarriers and the incorporation of growth limitation due to contact inhibition and cell metabolism. The model structure was chosen due to its simple design and the possibility to extract all model parameters estimated from a few cultivations. The model is shown in Supplement, Table S1. Least square methods were used to determine the specific model parameters, which were used as initial values to determine the expected process variability. For this purpose, the model parameters were varied 1000-fold based on the experimental uncertainty (e.g., measurement error) and thus the measurement errors were simulated. Please see References [13,14] for further details.

### 2.6.2 | mDoE toolbox

The combination of a mathematical process model, including model-parametric uncertainties with the computational planning and evaluation of DoE designs are the main parts of the mDoE software toolbox. Please see References [33] and [42] for more details about the toolbox and its application. In brief, the biotechnological system is modeled first based on the objective of the study. After defining the mathematical model, Monte-Carlo based parametric uncertainties are derived and, process variability is simulated to be later used in the DoE evaluation. Experimental factors and responses are defined as well as a DoE design is subsequently planned. For each recommended factor combination, the time courses of the modeled state variables are simulated multiple times and used for the computational evaluation. The design plan is analyzed, and response surface plots are generated automatically for visualization and experiments are recommended to be performed. After defining the response surface plots, user-defined constraints are chosen and the desirability function is calculated for each response individually. With the desirability function the multidimensional optimization problem is standardized to just one desirability function, which will be reduced with the multiplication of the different desirability function values to one overall desirability. The desirability is 0 if the optimization criteria is not fulfilled and the desirability tends toward 1 if the optimization is highly desirable.

# 3 | RESULTS AND DISCUSSION

The aim of this study was the evaluation of the applicability of the mDoE workflow for the development of an expansion process for

hMSC-TERT cells with only a limited amount of prior knowledge at a very early stage of development. First, suitable microcarriers for expansion in shake flasks were screened and the differentiation of the cells according to ISCT-guidelines was proven. Second, initial experiments were performed to generate prior knowledge and determine cause-effect relationships. Finally, the model parameters of the mathematical process model were adapted and the mDoE was used to determine the start time of the bead-to-bead transfer and the concentration of MC in the bead-to-bead transfer focusing on a maximum cell concentration.

## 3.1 | Characterization of MSCs and microcarrier-screening

### 3.1.1 | Characterization of hMSC-TERT

According to the ISCT guidelines, MSCs are characterized by plastic adherence, differentiation into adipocytes, chondrocytes and osteoblasts as well as the expression of certain surface markers.[46] Plastic adherence was confirmed by T-flasks cultures (not specifically shown). As can be seen in Figure 1 (Part I A), osteocyte differentiation was successfully demonstrated with alizarin red staining of intracellular calcium deposits. Differentiated adipocytes were confirmed by oil red O staining of the lipid vacuoles (Figure 1, Part I, B). Alcian blue staining of proteoglycans was used to detect chondrogenic differentiation (Figure 1, Part I, C). Overall, differentiation into adipocytes, osteoblasts, and chondrocytes was demonstrated successfully.

Surface marker analysis of hMSC-TERT (passage 90) were done on Cytodex 3 MCs. The hMSC-TERTs were negative (<2%) for hematopoietic markers such as CD45, CD34, CD14, CD19, and HLA-DR and positive (>90%) for stromal markers such as CD73, CD105, and CD90. Overall, relevant surface markers, plastic adherence and differentiation of hMSC-TERT were successfully detected according to ISCT guidelines.[46]

### 3.1.2 | MC-screening

Despite many studies involving MSCs and microcarrier culture investigating various aspects of the culture process, there is no unified set of culture conditions for MSC microcarrier expansion. However, many different types of microcarriers exist, each with different particle sizes, as well as a different structures (i.e., solid bead, macroporous, enzymatically digestible), and coatings (fibronectin, collagen, gelatin). The selection of the appropriate microcarrier is a fundamental component of microcarrier/stirred-tank bioreactor cell expansion. Therefore, it is of importance that the optimal microcarrier is selected from the outset based on a stringent selection methodology.[47] The use of MSCs in allogeneic cell therapy requires a scalable, cost-efficient manufacturing process including a well-chosen MC (17). In this study, six different MC were investigated regarding the growth of hMSC-TERT cells and the fluorescence-stained images can be seen in Figure 2 with different magnification.

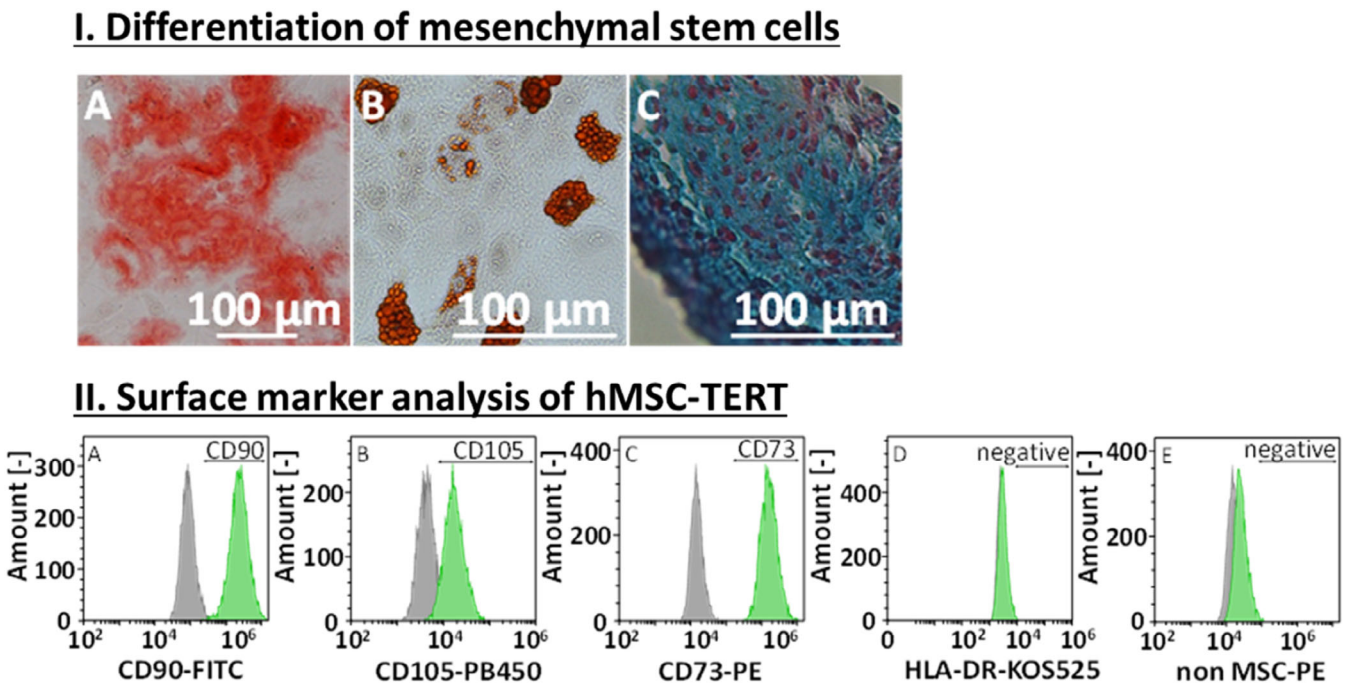


**FIGURE 1** Part I: Differentiation of mesenchymal stem cells into osteoblasts (A), adipocytes (B) and chondrocytes (C). Differentiation was performed in T-flasks (A, B) and conical centrifugation tubes (C) in differentiation medium. Alizarin red staining highlights calcium accumulation in osteoblasts (A), whereas lipids are stained in adipocytes by oil red OR staining (B). The aggrecan of the extracellular matrix is stained by Alcian blue and the nuclei with a nuclear red stain (C). Part II: Surface marker analysis of hMSC-TERT expanded on Cytodex 3-MCs in DMEM. Positive markers CD90, CD105, and CD73 (A-C) and the negative cocktail with CD45, CD34, CD14, CD19 (D), and HLA-DR (E). Isotype controls are shown in gray. hMSC-TERT of passage 90 were characterized.

As shown in Figure 2, the cells attach to all surfaces and different cell growth was observed for the MCs. Compared to the Collagen-Coated and Cytodex 3 MCs, the FACT, Plastic, PlasticPlus, and StarPlus MCs are sparsely overgrown. Smaller cell–cell-agglomerates and MC-cell-agglomerates were detected in the CollagenCoated MCs (Figure 2A). Only MC-cell-agglomerates were detected in Cytodex 3 MCs (Figure 2B). The FACT MC are barely overgrown, instead forming cell–cell-agglomerates up to 260 µm in size (Figure 2C). MC-cell-agglomerates are a typical phenomenon, as documented by Jossen et al.[44] and Abraham et al.,[21] among others. It was emphasized there that limitations occur due to the formation of concentration gradients within MC-cell-agglomerates. According to Abraham et al., these should be avoided.[21] Due to the efficient growth of hMSC-TERTs on Cytodex 3 MCs, they were further used in this study.

## 3.2 | Set-up of mathematical model

### 3.2.1 | Prior knowledge and determination of cause-effect relationships

The basis of mathematical process modeling is the determination of cause-effect relationships as previously published.[42] For hMSC-TERT, no dynamic cultivation data was available at the beginning of the study. To generate a first understanding about the dynamic cultivation behavior of hMSC-TERT, multiple shake flask growth cultures were experimentally performed. Based on our experience, typical medium components such as $c_{Glc}$, $c_{Gln}$, and $c_{MC}$ were examined since these have the main impact on the expansion process. The initial concentration of glucose ($c_{Glc,I}$) varied in the range of 5–60 mmol $L^{-1}$ and the initial concentration of glutamine ($c_{Gln,I}$) varied in the range of 2–12 mmol $L^{-1}$ based on our prior knowledge in the field of cell expansion processes.[32] The range of $c_{MC}$ was 1–5 g $L^{-1}$ based on previous studies.[42] In addition, the feasibility of bead-to-bead transfer was also tested. The investigated factors were the freshly added microcarriers ($c_{F,MC}$), which represents the percentage of added fresh MCs in relation to the initial medium concentration and the time of the addition ($t_{feed}$). Experiments were selected to best cover the expected experimental space based on our experience with adherent growing cells and typical medium components.

For comparison of the results, the growth rates up to the bead-to-bead transfer ($\mu_{max,before,btb}$) and after the bead-to-bead transfer ($\mu_{max,after,btb}$), the maximum cell number $X_{v,max}$ and the multiplication factor VF are summarized in Table 1.

By analyzing these six experiments the following cause-effect relationships were derived. The highest maximum cell numbers were

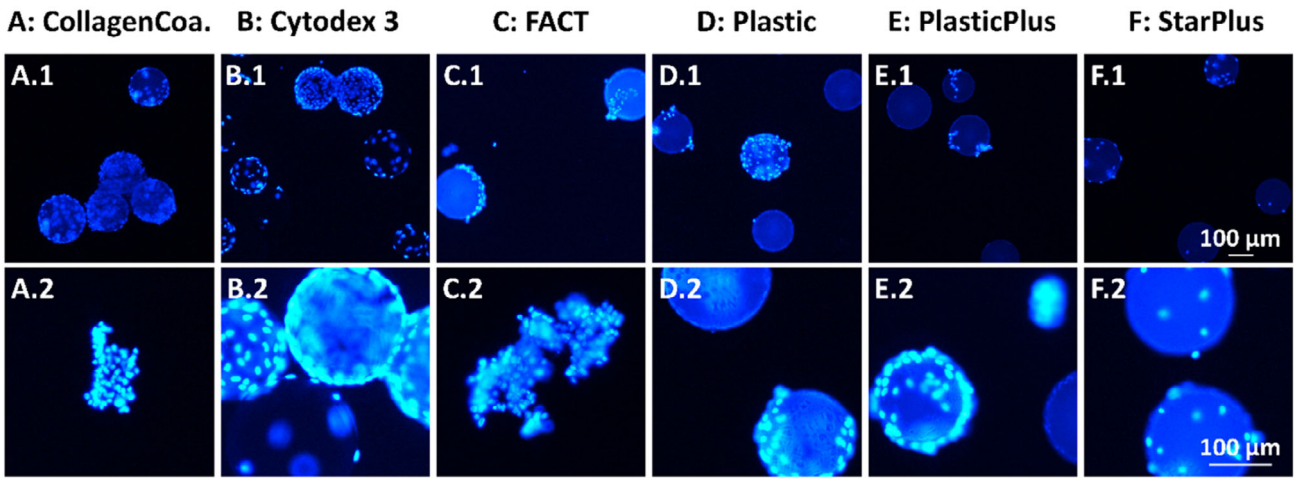


**FIGURE 2** Fluorescently stained SoloHill and Cytodex 3 MCs (A-CollagenCoated, B-Cytodex 3, C-FACT, D-Plastic, E-PlasticPlus, F-StarPlus). Fluorescence staining with DAPI, hMSC-TERT (Passage P92) were cultured for 72 h, see Section 2.1 for cultivation details.

**TABLE 1** Comparison of specific characteristic values as a function of MC concentration.

| Exp. | $c_{MC}$ [g $L^{-1}$] | $c_{Glc,I}$ [mmol $L^{-1}$] | $c_{Gln,I}$ [mmol $L^{-1}$] | $c_{F,MC}$ [%] | $t_{feed}$ [h] | $\mu_{max,before,btb}$ [$h^{-1}$] | $\mu_{max,after,btb}$ [$h^{-1}$] | $X_{V,max}$ [cells $cm^{-2}$] | VF [–] |
|---|---|---|---|---|---|---|---|---|---|
| 1 | 5 | 5,6 | 2 | - | - | - | - | 60,839 | 0.9 |
| 2 | 5 | 60 | 12 | 50 | 72 | 0.007 | 0.008 | 9345 | 1.3 |
| 3 | 5 | 5 | 12 | 50 | 120 | 0.012 | 0.011 | 8770 | 1.3 |
| 4 | 1 | 5 | 2 | 50 | 120 | 0.024 | 0.019 | 92,555 | 8.5 |
| 5 | 1 | 60 | 2 | 50 | 120 | 0.029 | 0.021 | 115,394 | 15.5 |
| 6 | 2.5 | 27.5 | 5 | 50 | 120 | 0.015 | 0.014 | 46,157 | 4.5 |

*Note*: Bead-to-bead transfer was performed after 120 h with a 100% medium and a 50% MC addition. Cells were innoculated with 5000 cells $cm^{-2}$ in each experiment. No Bead to Bead transfer was performed in experiment 1. The specific cultivation data can be seen in Figure S1.

achieved in Experiment 4 and Experiment 5 (Table 1) with an MC concentration of 1 g $L^{-1}$. Based on the determined growth rates, a mean maximum specific growth rate of $\mu_{max} = 0.027\ h^{-1}$ was assumed for the hMSC TERT cells with a $c_{MC} = 1\ g\ L^{-1}$ before bead-to-bead transfer. For all other $c_{MC}$, a decreased growth with an approximated reduction of $\mu_{max}$ by 30% was determined before and after bead-to-bead transfer (Exp. 2, 3, 6 in Table 1). Furthermore, a variation of $c_{Glc,I}$ and $c_{Gln,I}$ have only a small influence on cell growth. As long as both substrates are present, no limiting effects are present.

### 3.2.2 | Estimation of model parameters

Based on the determined cause-effect relationships, the model parameters were estimated for the experimental hMSC TERT cultivation data. A previously published mathematical model developed for adherent-growing L929 cells was used in this study to model the growth and main metabolism for hMSC TERT cells (see Table S1). Starting from this model, no differential equations had to be changed and only the initial parameters and the boundary conditions of the mathematical model were adjusted. To apply the uncertainty distribution in the mDoE toolbox, the initial values were varied 1000-fold by ±5% and the parameters were determined using Monte-Carlo simulations. The initial values and the estimated model parameters can be seen in Table 2.

To assess the goodness of the adapted mathematical model including the estimated model parameters, the model was used to simulate all experiments mentioned in Table 1 and the coefficient of determination was calculated for each simulated variable. As can be seen in Figure 3a,b, $X_v$ was simulated with a coefficient of determination ($R^2$) > 0.80. The data points are close to the identity line indicating a high representation of the simulated to the experimental data. The uptake of glucose and glutamine as main sources of energy can be expressed well with a $R^2$ of 0.85 ($c_{Glc}$) and 0.69 ($c_{Gln}$). Lactate, as main metabolic waste product, is described with $R^2 = 0.69$ (Figure 3e). No correlation was detected for the decrease in ammonium concentration, so this phenomenon was only simulated poorly and was not considered for the process development (Figure 3f).

## 3.3 | Process optimization with mDoE toolbox

Based on previously described results (Table 1), it was shown that a $c_{MC} = 1$ g/L led to improved cell growth. The aim of process optimization in this study was to identify the best start time of feeding of MC ($t_{feed}$) and an appropriate MC concentration ($c_{F,MC}$) in the feed. For this purpose, a mDoE was performed based on the previously introduced mathematical process model. The factor limits were set broadly so that a large experimental space was studied using the simulations. Freshly added MC during bead-to-bead transfer varied in the range of 25%, 50% and 100% (0.25–1 g $L^{-1}$) and the start time of the feed from 72 to 168 h. The minimum limit of the feed start time was set at 72 h to allow the cells to adhere to the MCs and to transition to the exponential phase. After 168 h, a transition to stationary phase was already observed in isolated cases, so this was set as the maximum limit. Additionally, $c_{Glc,I}$ was set to 12 mmol $L^{-1}$, $c_{Gln,I}$ to 4 mmol $L^{-1}$ and $c_{MC}$ to 1 g $L^{-1}$. A D-optimal experimental design was chosen as the experimental design, since effective experimental designs can be generated with a small number of factor combinations, as was shown in Reference [48].

Using mDoE, a response surface was predicted with a maximal desirability (maximizing cell concentration) to be at intermediate as well as maximum $c_{F,MC}$ and early to intermediate $t_{feed}$. For $c_{F,MC}$ lower than 0.6 g $L^{-1}$, a strong decrease in the desirability is predicted whereas the influence of $t_{feed}$ seems to be rather low. Out of the planned experimental conditions (blue points in Figure 4a), 6 conditions were chosen and experimentally tested (Figure 4b). The growth

**TABLE 2** Initial values and estimated model parameters; numerical values show average and standard deviation of model parameters, the microcarrier concentration was considered as shown in Table S2.

| Parameter | Unit | Initial value | Estimated model parameters |
|---|---|---|---|
| $\mu_{d,max}$ | $h^{-1}$ | 0.02 | 0.008 ± 0.002 |
| $\mu_{d,min}$ | $10^{-4}\ h^{-1}$ | 0.003 | 0.0002 ± 0.002 |
| $\mu_{max}$ | $h^{-1}$ | 0.02 | 0.013 ± 0.0005 |
| $K_{att,max}$ | $h^{-1}$ | 0.03 | 0.053 ± 0.003 |
| $K_{d,LS}$ | mmol $L^{-1}$ | 0.005 | 0.03 ± 0.004 |
| $K_{Glc}$ | mmol $L^{-1}$ | 0.19 | 0.25 ± 0.02 |
| $K_{Gln}$ | mmol $L^{-1}$ | 2.5 | 5.43 ± 0.46 |
| $k_{s,LS}$ | mmol $L^{-1}$ | 0.01 | 0.002 ± 0.0002 |
| $k_{LS}$ | mmol $L^{-1}$ | 0.1 | 0.03 ± 0.003 |
| $Y_{X/Glc}$ | $10^7$ cells $L^{-1}$ $mmol^{-1}$ | 7.2 | 2 ± 0.2 |
| $Y_{X/Gln}$ | $10^8$ cells $L^{-1}$ $mmol^{-1}$ | 1.7 | 6 ± 0.6 |
| $q_{LS,max}$ | $10^{-11}$ mmol $cell^{-1}$ $h^{-1}$ | 1.4 | 9 ± 1 |
| $Y_{Lac/Glc}$ | - | 1.5 | 2.5 ± 0.2 |
| $Y_{amm/Gln}$ | - | 0.6 | 0.6 ± 0.09 |

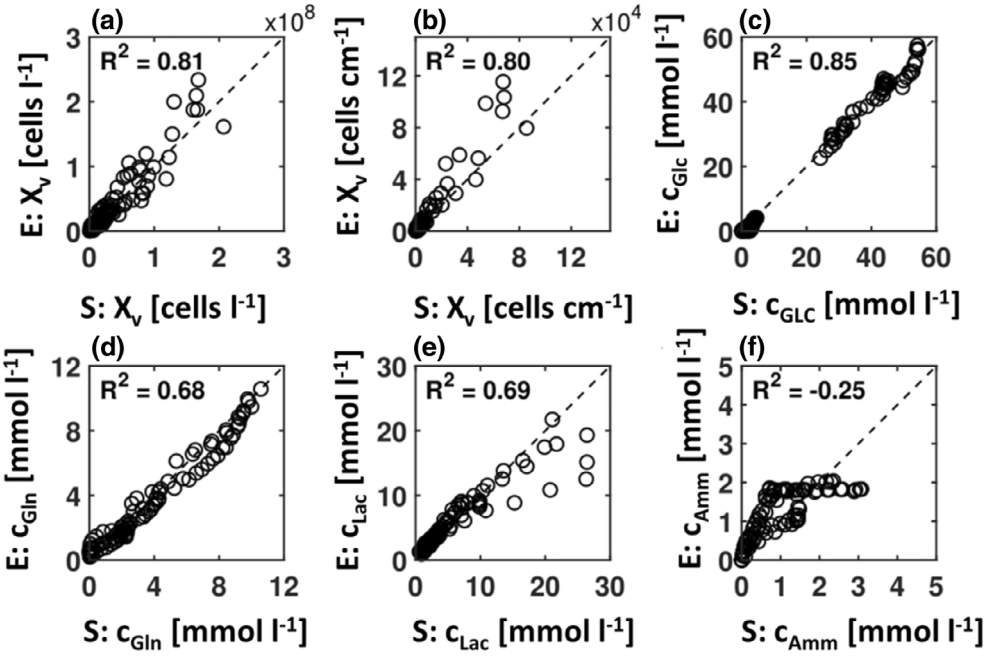


**FIGURE 3** Comparison of experimentally measured data (E-experimental) to simulated data (S-simulation) for the 6 experiments mentioned in Table 1. The identity line (dashed) is given as reference. Statistical information ($R^2$) is presented for all curves.

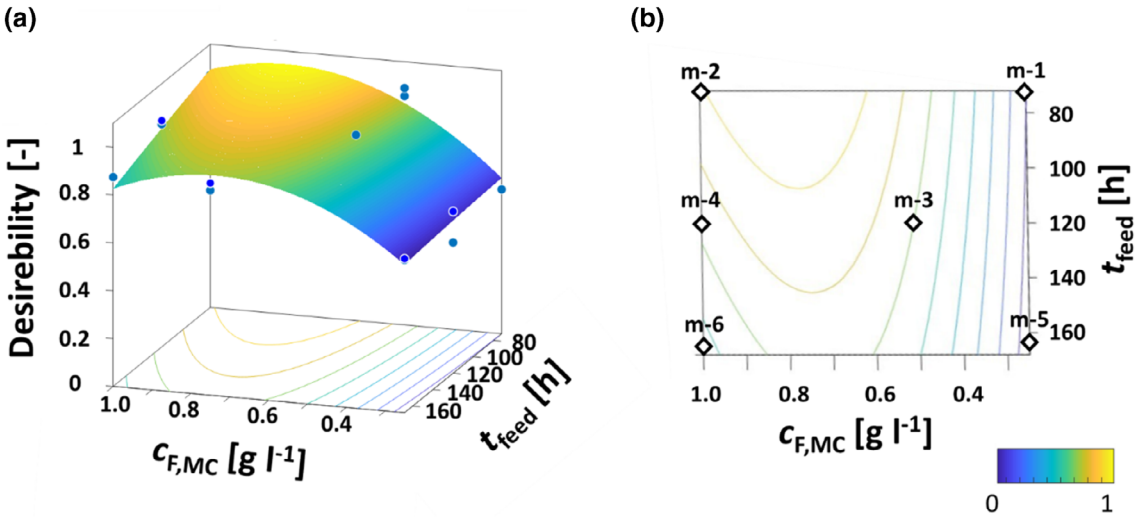


**FIGURE 4** (a) Response surface plot of mDoE for the optimization of $c_{F,MC}$ and $t_{feed}$, blue points are simulated experimental conditions for mDoE, the surface is simulated. (b) contour plot of $c_{F,MC}$ and $t_{feed}$, experimentally implemented conditions (m means mDoE).

curves can be seen in Figure 5 A with different characteristic behavior. For m-1 (low $c_{F,MC}$ and low $t_{feed}$), cells grew up to a maximum of $14.5 \times 10^4$ cells cm$^{-2}$ at 312 h. For the next hours the cell number declined to $12.7 \times 10^4$ cells cm$^{-2}$. A low $t_{feed}$ and a high $c_{F,MC}$ (Figure 5, m-2) resulted in a higher $X_v = 17.5 \times 10^4$ cells cm$^{-2}$ at 360 h and an average $t_{feed}$ and $c_{F,MC}$ (Figure 5, m-3) led to a little bit smaller maximal $X_v = 15.2 \times 10^4$ cells cm$^{-2}$. The lowest maximal cell number of $9.1 \times 10^4$ cells cm$^{-2}$ was achieved for an average $t_{feed}$ and high $c_{F,MC}$ (Figure 5, m-4) whereas the highest $X_v = 18.8 \times 10^4$ cells cm$^{-2}$ was determined for a high $t_{feed}$ and a low $c_{F,MC}$ (Figure 5, m-5). For a high $t_{feed}$ and $c_{F,MC}$, an rather low $X_v = 10.9 \times 10^4$ cells cm$^{-2}$ was measured (Figure 5, m-6). $c_{Glc}$ and $c_{Gln}$ was steadily taken up by the cells during growth and $c_{Glc}$ was consumed after 360 h of cultivation. $c_{Gln}$ was given in excess and was not fully consumed. Overall, a low $c_{F,MC}$ and a late $t_{feed}$ is recommended for an efficient cell expansion, as was tested in experiment m-5. Additionally, this results showed that $c_{F,MC}$ <1 g L$^{-1}$ are not yet optimally described with the mathematical model. Modifications would be necessary for further usage. However, this corresponds to the concept of the mDoE, to increase the process knowledge in a short time with a smaller number of experiments.

All in all, before bead-to-bead transfer, a maximum cell concentration up to $4 \times 10^4$ cells cm$^{-2}$ (m-3) and $5.25 \times 10^4$ cells cm$^{-2}$ (m-5) could be reached. After bead-to-bead transfer, a maximum cell concentration of $18.8 \times 10^4$ cells cm$^{-2}$ was achieved after 360 h of cultivation (m-5). Leber et al.[28] investigated the growth of hMSC-TERT cells using different microcarriers. They reported a maximal cell concentration of $3 \times 10^4$ cells cm$^{-2}$ in spinner cultures using glass-coated

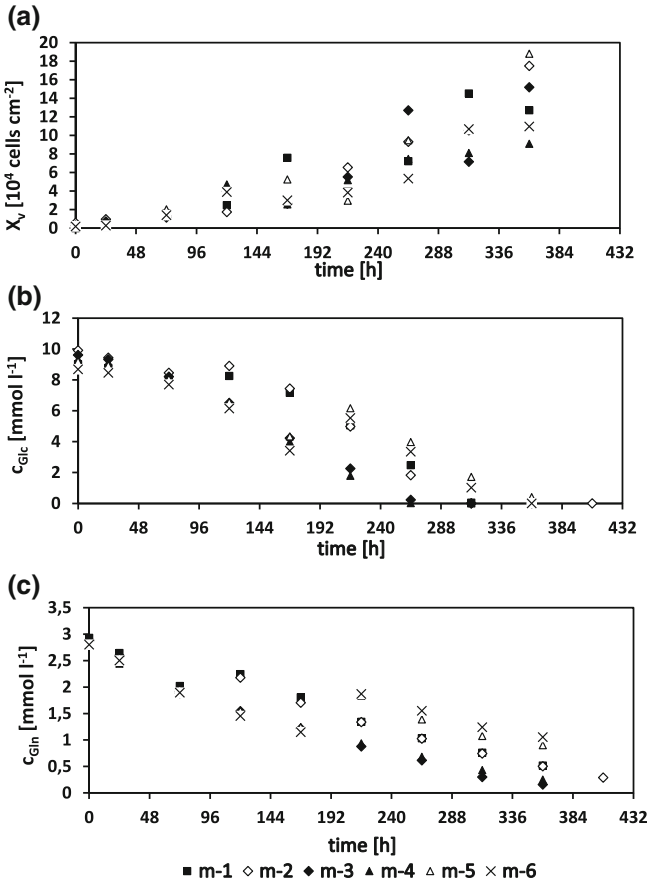


**FIGURE 5** Experimentally tested cultivations, based on Figure 4b.

microcarriers (Solohill Glass Coated, Pall), both before and after bead-to-bead transfer. In comparison to this maximal cell number, a slightly higher cell yield was achieved here before bead-to-bead transfer (m-3 and m-5). After bead-to-bead transfer, up to 6 times more cells per $cm^2$ were cultivated in m-5 using different microcarriers and an optimized bead-to-bead transfer protocol.

Additionally, it is important to highlight the successful cultivation of hMSC-TERT-cells on microcarriers under shake flask conditions. So far, mostly spinner cultures have been reported for small scale suspension cultures of hMSC-TERT cells. Wyrobnik et al.[49] summarized cell expansion processes in stirred tank bioreactors with a typical range of cell densities between $1 \times 10^5$ cells $mL^{-1}$ and $1 \times 10^6$ cells $mL^{-1}$ and a cell viability above 90% $\times$ $10^6$ cells $mL^{-1}$ (converted from cell $cm^{-2}$ to cells $mL^{-1}$), which is comparable to the previously described range in stirred tank bioreactors. Therefore, the small-scale expansion in shake flasks is an appropriate tool for process development and investigation.

## 4 | CONCLUSION

The objective of this research was to assess the efficacy of using the mDoE concept in enhancing the expansion processes for ATMPs, such as MSC cells. To achieve this, a workflow for model-assisted process development was set up. First, various microcarriers were compared, and Cytodex 3 microcarriers were selected for further cultivation due to their favorable handling characteristics. The study then progressed by elaborating cause-effect relationships based on six preliminary experiments. These relationships were utilized to define the parameters of a mathematical model, forming the basis for implementing the mDoE. By utilizing the mDoE approach, the range of possible experimental was narrowed down. This facilitated the optimization of parameters like feeding rate ($t_{feed}$) and microcarrier concentration ($c_{F,MC}$) through six additional experiments only.

This optimization process led to a significant increase in cell yield compared to existing literature. It is noteworthy that the successful results were accomplished without the need for iterative DoE cycles. This was possible due to a comprehensive analysis of cultivation data and a refined iterative modification of the mathematical process model. Consequently, only experiments that held substantial informational value were conducted, leading to a reduction in the time required for optimizing the bead-to-bead transfer process. With focus on the manufacturing of ATMPs, which often demands tailored, individualized processing, a significantly reduced effort for processes is essential, setting it apart from the production of traditional biopharmaceuticals. Utilizing the mDoE techniques holds significant promise in harnessing a wide array of diverse data and knowledge sources. This, in turn, contributes to an enhanced comprehension of cell culture methodologies and has the potential to accelerate the progression through the clinical development phases, thus speeding up the market entry of ATMPs.

## NOMENCLATURE

### List of Symbols

| | |
|---|---|
| $c_{Amm}$, [mmol $L^{-1}$] | concentration of ammonia |
| $c_{F,MC}$, [g $L^{-1}$] | freshly added microcarriers |
| $c_{Glc}$, [mmol $L^{-1}$] | concentration of glucose |
| $c_{Glc,I}$, [mmol $L^{-1}$] | initial glucose concentration |
| $c_{Gln}$, [mmol $L^{-1}$] | concentration of glutamine |
| $c_{Gln,I}$, [mmol $L^{-1}$] | initial glutamine concentration |
| $c_{MC}$, [g $L^{-1}$] | concentration of microcarrier |
| $c_{Lac}$, [mmol $L^{-1}$] | concentration of lactate |
| $c_{LS}$, [mmol $L^{-1}$] | concentration of limiting substrate |
| $k_{att}$, [$h^{-1}$] | attachment constant |
| $K_{S,LS}$, [mmol $L^{-1}$] | kinetic parameter |
| $K_{d,LS}$, [mmol $L^{-1}$] | kinetic parameter |
| $q_{Glc}$, [mmol $cell^{-1}$ $h^{-1}$] | cell specific uptake rate of glucose |
| $q_{Gln}$, [mmol $cell^{-1}$ $h^{-1}$] | cell specific uptake rate of glutamine |
| $R^2$, [–] | coefficient of determination |
| $t_{feed}$, [h] | time of the microcarrier addition |
| VF, [–] | multiplication factor |
| $V_{PBS}$, [mL] | volume PBS |
| $V_{Medium}$, [mL] | volume Medium |
| $V_{Trypsin}$, [mL] | volume Trypsin |
| $X_{Inokulum}$, [cells $cm^{-2}$] | inoculation cell concentration |
| $X_V$, [cells $cm^{-2}$] | cells growing on microcarrier |
| $X_{v,max}$, [cells $cm^{-2}$] | maximum cell number |
| $X_{SUS}$, [cells $mL^{-1}$] | cells growing in suspension |

| | |
|---|---|
| $Y_{X/Glc}$, [cells mmol$^{-1}$] | ratio of growth to cell yield for glucose |
| $Y_{X/Gln}$, [cells mmol$^{-1}$] | ratio of growth to cell yield for glutamine |

**Greek Symbols**

| | |
|---|---|
| $\mu$, [h$^{-1}$] | specific growth rate |
| $\mu_d$, [h$^{-1}$] | specific death rate |
| $\mu_{d,min}$, [h$^{-1}$] | minimum death rate |
| $\mu_{d,max}$, [h$^{-1}$] | maximum death rate |
| $\mu_{max}$, [h$^{-1}$] | maximum growth rate |
| $\mu_{max,before,btb}$, [h$^{-1}$] | growth rates up to the bead-to-bead transfer |
| $\mu_{max,after,btb}$, [h$^{-1}$] | growth rate after the bead-to-bead transfer |

## AUTHOR CONTRIBUTIONS

**Johannes Möller:** Conceptualization; software; project administration; writing – original draft; visualization; investigation. **Kim B. Kuchemüller:** Investigation; writing – original draft; methodology; software; data curation; visualization; conceptualization. **Ralf Pörtner:** Conceptualization; project administration; supervision; resources; writing – review and editing; investigation.

## ACKNOWLEDGMENTS

Prof. Dr. M. Kassem, Southern Danish University, Denmark and Prof. Dr.-Ing. D. Salzig, Technische Hochschule Mittelhessen, Germany. Dr.-Ing. Kim B. Kuchemüller was funded by a Scholarship Awarded on the basis of the Hamburg Promotion of Scientific and Artistic Talent Act. Open Access funding enabled and organized by Projekt DEAL.

## CONFLICT OF INTEREST STATEMENT

The authors declare no competing interests.

## DATA AVAILABILITY STATEMENT

The data that support the findings of this study are available on request from the corresponding author. The data are not publicly available due to privacy or ethical restrictions.

## ORCID

*Johannes Möller* https://orcid.org/0000-0001-9546-055X

## REFERENCES

1. Goula A, Gkioka V, Michalopoulos E, et al. Advanced therapy medicinal products challenges and perspectives in regenerative medicine. *J Clin Med Res*. 2020;12(12):780-786. doi:10.14740/jocmr3964
2. Seoane-Vazquez E, Shukla V, Rodriguez-Monguio R. Innovation and competition in advanced therapy medicinal products. *EMBO Mol Med*. 2019;11(3):e9992. doi:10.15252/emmm.201809992
3. Iglesias-Lopez C, Agustí A, Vallano A, Obach M. Current landscape of clinical development and approval of advanced therapies. *Mol Ther Methods Clin Dev*. 2021;23:606-618. doi:10.1016/j.omtm.2021.11.003
4. Guedan S, Ruella M, June CH. Emerging cellular therapies for cancer. *Annu Rev Immunol*. 2019;37:145-171. doi:10.1146/annurev-immunol-042718-041407
5. Lin H, Cheng J, Mu W, Zhou J, Zhu L. Advances in universal CAR-T cell therapy. *Front Immunol*. 2021;12:744823744823. doi:10.3389/fimmu.2021.744823
6. Elbuluk A, Einhorn TA, Iorio R. A comprehensive review of stem-cell therapy. *JBJS Rev*. 2017;5(8):e15e15. doi:10.2106/JBJS.RVW.17.00002
7. Pörtner R, Parida SK, Schaffer C, Hoffmeister H. Landscape of manufacturing process of ATMP cell therapy products for unmet clinical needs. In: Sharma R, ed. *Stem Cells in Clinical Practice and Tissue Engineering*. Intech Open; 2018.
8. Jung S, Panchalingam KM, Rosenberg L, Behie LA. Ex vivo expansion of human mesenchymal stem cells in defined serum-free media. *Stem Cells Int*. 2012;2012:123030123030. doi:10.1155/2012/123030
9. Heathman TR, Rafiq QA, Chan AK, et al. Characterization of human mesenchymal stem cells from multiple donors and the implications for large scale bioprocess development. *Biochem Eng J*. 2016;108:14-23. doi:10.1016/j.bej.2015.06.018
10. Han F, Wang J, Ding L, et al. Tissue engineering and regenerative medicine: achievements, future, and sustainability in Asia. *Front Bioeng Biotechnol*. 2020;8:83. doi:10.3389/fbioe.2020.00083
11. Ramos T, Moroni L. Tissue engineering and regenerative medicine 2019: the role of biofabrication-a year in review. *Tissue Eng Part C Methods*. 2020;26(2):91-106. doi:10.1089/ten.tec.2019.0344
12. Wardhana A, Valeria M. Tissue engineering and regenerative medicine: a review. *J Plast Rekons*. 2020;7(1):10-17. doi:10.14228/jpr.v7i1.278
13. Aijaz A, Li M, Smith D, et al. Biomanufacturing for clinically advanced cell therapies. *Nat Biomed Eng*. 2018;2(6):362-376. doi:10.1038/s41551-018-0246-6
14. Iyer RK, Bowles PA, Kim H, Dulgar-Tulloch A. Industrializing autologous adoptive immunotherapies: manufacturing advances and challenges. *Front Med (Lausanne)*. 2018;5:150. doi:10.3389/fmed.2018.00150
15. Möller J, Pörtner R. Digital twins for tissue culture techniques—concepts, expectations, and state of the art. *Processes*. 2021;9(3):447. doi:10.3390/pr9030447
16. Fernández A, Navarro-Zapata A, Escudero A, et al. Optimizing the procedure to manufacture clinical-grade NK cells for adoptive immunotherapy. *Cancers (Basel)*. 2021;13(3):577. doi:10.3390/cancers13030577
17. Elseberg C, Leber J, Weidner T, Czermak P. The challenge of human mesenchymal stromal cell expansion: current and prospective answers. *New Insights into Cell Culture Technology*. IntechOpen; 2017.
18. Hewitt C, Lee K, Nienow A, Thomas R, Smith M, Thomas C. Expansion of human mesenchymal stem cells on microcarriers. *Biotechnol Lett*. 2011;33:2325-2335.
19. Jossen V, Eibl D, Eibl R. Numerical methods for the design and description of in vitro expansion processes of human mesenchymal stem cells. *Adv Biochem Eng Biotechnol*. 2021;177:185-228. doi:10.1007/10_2020_147
20. van den Bos C, Keefe R, Schirmaier C, McCaman M. Therapeutic human cells: manufacture for cell therapy/regenerative medicine. *Adv Biochem Eng Biotechnol*. 2014;138:61-97. doi:10.1007/10_2013_233
21. Abraham E, Gupta S, Jung S, McAfee E. Chapter 6—bioreactor for scale-up: process control. In: Viswanathan S, Hematti P, eds. *Mesenchymal Stromal Cells*. Academic Press; 2017:139-178.
22. Rowley J, Abraham E, Campbell A, Brandwein H, Oh S. Meeting lot-size challenges of manufacturing adherent cells for therapy. *BioProcess Int*. 2012;10(3):7. https://bioprocessintl.com/manufacturing/cell-therapies/meeting-lot-size-challenges-of-manufacturing-adherent-cells-for-therapy-328093/
23. Jossen V, Schirmer C, Mostafa Sindi D, et al. Theoretical and practical issues that are relevant when scaling up hMSC microcarrier production processes. *Stem Cells Int*. 2016;2016:47604144760414. doi:10.1155/2016/4760414
24. Kaiser SC, Kraume M, Eibl D, Eibl R. Single-use bioreactors for animal and human cells. In: Al-Rubeai M, ed. *Animal Cell Culture*. Springer; 2015:445-500.
25. Schnitzler AC, Verma A, Kehoe DE, et al. Bioprocessing of human mesenchymal stem/stromal cells for therapeutic use: current technologies and challenges. *Biochem Eng J*. 2016;108:3-13. doi:10.1016/j.bej.2015.08.014

26. Tekkatte C, Gunasingh GP, Cherian KM, Sankaranarayanan K. "Humanized" stem cell culture techniques: the animal serum controversy. *Stem Cells Int*. 2011;2011:504723504723. doi:10.4061/2011/504723
27. Panchalingam KM, Jung S, Rosenberg L, Behie LA. Bioprocessing strategies for the large-scale production of human mesenchymal stem cells: a review. *Stem Cell Res Ther*. 2015;6:225. doi:10.1186/s13287-015-0228-5
28. Leber J, Barekzai J, Blumenstock M, Pospisil B, Salzig D, Czermak P. Microcarrier choice and bead-to-bead transfer for human mesenchymal stem cells in serum-containing and chemically defined media. *Process Biochem*. 2017;59:255-265. doi:10.1016/j.procbio.2017.03.017
29. Trias E, Juan M, Urbano-Ispizua A, Calvo G. The hospital exemption pathway for the approval of advanced therapy medicinal products: an underused opportunity? The case of the CAR-T ARI-0001. *Bone Marrow Transplant*. 2022;57(2):156-159. doi:10.1038/s41409-021-01463-y
30. Mandenius C-F, Brundin A. Bioprocess optimization using design-of-experiments methodology. *Biotechnol Progress*. 2008;24(6):1191-1203. doi:10.1002/btpr.67
31. Parampalli A, Eskridge K, Smith L, Meagher MM, Mowry MC, Subramanian A. Developement of serum-free media in CHO-DG44 cells using a central composite statistical design. *Cytotechnology*. 2007;54(1):57-68. doi:10.1007/s10616-007-9074-3
32. Möller J, Kuchemüller KB, Steinmetz T, Koopmann KS, Pörtner R. Model-assisted Design of Experiments as a concept for knowledge-based bioprocess development. *Bioprocess Biosyst Eng*. 2019;42(5):867-882. doi:10.1007/s00449-019-02089-7
33. Moser A, Kuchemüller KB, Deppe S, et al. Model-assisted DoE software: optimization of growth and biocatalysis in Saccharomyces cerevisiae bioprocesses. *Bioprocess Biosyst Eng*. 2021;44(4):683-700. doi:10.1007/s00449-020-02478-3
34. Kuchemüller KB, Pörtner R, Möller J. Efficient optimization of process strategies with model-assisted Design of Experiments. *Methods Mol Biol*. 2020;2095:235-249. doi:10.1007/978-1-0716-0191-4_13
35. von Stosch M, Hamelink J-M, Oliveira R. Hybrid modeling as a QbD/PAT tool in process development: an industrial E. Coli case study. *Bioprocess Biosyst Eng*. 2016;39(5):773-784. doi:10.1007/s00449-016-1557-1
36. Bayer B, Duerkop M, Pörtner R, Möller J. Comparison of mechanistic and hybrid modeling approaches for characterization of a CHO cultivation process: requirements, pitfalls and solution paths. *Biotechnol J*. 2023;18(1):e2200381e2200381. doi:10.1002/biot.202200381
37. Abt V, Barz T, Cruz-Bournazou MN, et al. Model-based tools for optimal experiments in bioprocess engineering. *Curr Opin Chem Eng*. 2018;22(6):244-252. doi:10.1016/j.coche.2018.11.007
38. Siebertz K, van Bebber D, Hochkirchen T. *Statistische Versuchsplanung: Design of Experiments (DoE)*. Springer; 2010.
39. Herwig C, Pörtner R, Möller J. *Digital Twins: Tools and Concepts for Smart Biomanufacturing*. Springer International Publishing; 2021.
40. Herwig C, Pörtner R, Möller J. *Digital Twins: Applications to the Design and Optimization of Bioprocesses*. Springer International Publishing; 2021.
41. Geris L, Lambrechts T, Carlier A, Papantoniou I. The future is digital: in silico tissue engineering. *Current Opinion in Biomedical Engineering*. 2018;6:92-98. doi:10.1016/j.cobme.2018.04.001
42. Kuchemüller KB, Pörtner R, Möller J. Design of cell expansion processes for adherent-growing cells with mDoE-workflow. *Eng Life Sci*. 2023;23(5):e2200059e2200059. doi:10.1002/elsc.202200059
43. Rafiq QA, Brosnan KM, Coopman K, Nienow AW, Hewitt CJ. Culture of human mesenchymal stem cells on microcarriers in a 5 l stirred-tank bioreactor. *Biotechnol Lett*. 2013;35(8):1233-1245. doi:10.1007/s10529-013-1211-9
44. Jossen V, van den Bos C, Eibl R, Eibl D. Manufacturing human mesenchymal stem cells at clinical scale: process and regulatory challenges. *Appl Microbiol Biotechnol*. 2018;102(9):3981-3994. doi:10.1007/s00253-018-8912-x
45. Pörtner R, Schäfer T. Modelling hybridoma cell growth and metabolism—a comparison of selected models and data. *J Biotechnol*. 1996;49(1–3):119-135. doi:10.1016/0168-1656(96)01535-0
46. Dominici M, Le Blanc K, Mueller I, et al. Minimal criteria for defining multipotent mesenchymal stromal cells. The International Society for Cellular Therapy position statement. *Cytotherapy*. 2006;8(4):315-317. doi:10.1080/14653240600855905
47. Rafiq QA, Coopman K, Nienow AW, Hewitt CJ. Systematic microcarrier screening and agitated culture conditions improves human mesenchymal stem cell yield in bioreactors. *Biotechnol J*. 2015;11:473-486. doi:10.1002/biot.201400862
48. Kuchemüller KB, Pörtner R, Möller J. Digital twins and their role in model-assisted Design of Experiments. *Adv Biochem Eng Biotechnol*. 2021;177:29-61. doi:10.1007/10_2020_136
49. Wyrobnik TA, Ducci A, Micheletti M. Advances in human mesenchymal stromal cell-based therapies—towards an integrated biological and engineering approach. *Stem Cell Res*. 2020;47:101888101888. doi:10.1016/j.scr.2020.101888


## SUPPORTING INFORMATION

Additional supporting information can be found online in the Supporting Information section at the end of this article.

**How to cite this article:** Kuchemüller KB, Pörtner R, Möller J. Implementation of mDoE-methods to a microcarrier-based expansion processes for mesenchymal stem cells. *Biotechnol. Prog*. 2024;40(3):e3429. doi:10.1002/btpr.3429